A fullerene–distyrylbenzene photosensitizer for two-photon promoted singlet oxygen production†

Elisabetta Collini, Ilaria Fortunati, Sara Scolaro, Raffaella Signorini, Camilla Ferrante,* Renato Bozio, Graziano Fabbrini, Michele Maggini,* Emiliano Rossi and Simone Silvestrini

Received 30th October 2009, Accepted 12th February 2010
First published as an Advance Article on the web 17th March 2010
DOI: 10.1039/b922740g

Novel compounds endowed with a high two-photon absorption (TPA) cross-section and a high singlet oxygen quantum yield, are sought after for their possible application in anti-cancer therapies. In this paper we present a prototype macromolecule bearing a distyrylbenzene dimer as TPA unit and a [60]fullerene moiety for singlet oxygen generation. Linear absorption and emission spectra are measured, to help understanding the interactions between the single molecular units. The TPA absorption properties of the distyrylbenzene alone as well as bound to the methanofullerene unit are recorded with the TPA-induced fluorescence technique. An appreciable enhancement of the TPA cross-section was observed in the molecular conjugate.

Singlet oxygen generation has been detected exciting the sample both in the Vis and NIR through one- and two-photon absorption processes, respectively. Although functionalization decreases the overall singlet oxygen quantum yield of fullerene, the presence of the distyrylbenzene antenna allows two-photon generation of singlet oxygen through an energy transfer process.

Introduction

Functionalized fullerenes are extensively studied as active components in photonic devices, such as, for instance, polymer solar cells[1–5] or optical limiters[6,7] for their strong electron accepting properties and weak ground state absorption which, in turn, is coupled to a strong absorption of excited singlet and triplet states in the whole visible range.[8,9] For the mentioned applications, a large number of derivatives have been considered, in particular fulleropyrrolidines and methanofullerenes, for their ease of synthesis and further functionalization.[10–12] A wide variety of donor-linked fullerenes with porphyrins,[13–19] tetrathiafulvalenes[20–23] or ferrocenes[24,25] have been prepared and studied in the past. More recently, several dyad systems, where [60]fullerene is combined with carbazole, benzothiazole, benzothiazole-triphenylammine[26,27] and diphenylammino-fluorene[28–30] moieties as well as distyrylbenzene[31] and oligo-(*p*-phenylene vinylene),[32–34] have been synthesised to serve as building blocks for photonic materials.

Water-soluble fullerenes and fullerene–polymer hybrids have, instead, been prepared specifically as sensitizers for singlet oxygen generation[35–40] in photodynamic therapy (PDT). PDT is a medical treatment that makes use of reactive oxygen species like singlet oxygen ($^1O_2$) and superoxide ($O_2^{\bullet -}$) as powerful oxidizing agents in cancer therapy,[41] ophthalmology[42] and dermatology.[43] Most photosensitizers, in medically-approved PDT applications, are tetrapyrrole-based compounds (porphyrins, chlorines, phthalocyanines). Similar to these traditional photosensitizers, excitation of functionalized fullerenes in oxygenated solutions leads to extremely efficient $^1O_2$ generation with an almost unitary quantum yield,[44] through an energy transfer process from the excited triplet state of the fullerene.[45,46] Recent reports have shown that in polar solvents, especially those containing reducing agents, illumination can also generate $O_2^{\bullet -}$.[47] Singlet oxygen and superoxide pathways are analogous to the Type II and Type I photochemical mechanisms identified in PDT with conventional tetrapyrrolic compounds.[48,49]

The biological activity of fullerenes in PDT has been known for more than a decade.[36] Several studies reported in the literature have demonstrated that fullerene-based photosensitizers could lead to DNA cleavage,[50] photoinactivation of viruses,[51] production of oxidative damage in membranes,[52] and even PDT-induced regression of tumors in mice.[53]

Recently, the two-photon absorption (TPA) process has been explored as an intriguing route to excite the photosensitizer for singlet oxygen generation. This strategy could improve many aspects of PDT: (i) the sample is excited by simultaneous absorption of two lower energy photons in the NIR region (750–900 nm) rather than with one higher energy photon in the Vis region (375–450 nm); excitation in the NIR region where the "transparency window" of skin falls, allows for deeper penetration in the tissues (hundreds of microns); (ii) absorption occurs only in the focal region of the beam, and therefore singlet oxygen can be produced only in a well defined volume of the sample, (iii) although not yet fully demonstrated, photobleaching of the sensitizing chromophore should be minimized.[54,55]

Department of Chemical Sciences and UdR INSTM, University of Padova, Via Marzolo 1, I-35131 Padova, Italy. E-mail: camilla.ferrante@unipd.it, michele.maggini@unipd.it; Fax: 00390498275239; Tel: 00390498275148

† Electronic supplementary information (ESI) available: Selected analytical and photophysical data for the investigated compounds. See DOI: 10.1039/b922740g

Currently, most of the molecular systems investigated as potential TPA photosensitizers are molecules showing a high TPA cross section, such as distyrylbenzenes (DSB)[56,57] or porphyrin dimers.[58] Porphyrin derivatives were also recently tested as photosensitizers for two-photon excited photodynamic therapy (TPE-PDT) *in vivo*. In particular TPE-PDT was successfully employed in the treatment of lung cancer, leading to tumor regression at a significant tissue depth,[59] and in the targeted closure of blood vessels associated with neoplastic diseases.[60]

In the search of molecules characterized both by high TPA cross sections and high singlet oxygen quantum yields, we propose the fullerene–distyrylbenzene conjugate (**1**). The idea is to functionalize the fullerene unit, characterized by a unitary singlet oxygen photosensitization quantum yield, with suitable chromophores capable of efficient TPA, acting as antennas. After TPA, the antenna (donor) transfers its excitation *via* energy transfer to the fullerene, where inter-system crossing and singlet oxygen generation occurs. This approach is particularly versatile because it demonstrates that by employing different chromophores or functional groups, with specialized functions, it is possible to generate new molecular conjugates endowed with targeted properties. Compound **1** is the first prototype that, although not yet optimized, still shows the basic properties, *i.e.* mildly efficient TPA that gives rise to appreciable singlet oxygen production, necessary for our purpose. Indeed amelioration of the present design should encompass an increase of the TPA cross-section as well as an improvement of the water solubility for application in the biomedical field.

Results and discussion

Synthesis

Methanofullerene **1** was synthesized in 30% yield through a nucleophilic cyclopropanation reaction to [60]fullerene of the iodomalonate anion that was formed *in situ* from malonate **4** and iodine in the presence of the base 1,8-diazabicyclo-[5.4.0]undec-7-ene (DBU, Scheme 1).[64] HPLC analysis was employed to assess the purity of **1**, whereas NMR spectroscopy (Fig. S9–S10)† and mass determination validate its proposed molecular structure. The *trans–trans* configuration of the double bonds in the distyrylbenzene moieties was established *via* NMR, through measurement of the $^3J_{HH}$ of the olefin protons which was found to be around 16 Hz, as reported in the literature.[65] Malonate **4** was, in turn, prepared in 45% overall yield as illustrated in Scheme 2. The Horner-Emmons Wittig (HEW) coupling reaction of *p*-methoxybenzaldehyde with 2,5-Bis(diethylphosphonate)-1,4-dimethoxybenzene[61] gave the *trans*-stylbene derivative **2** in 62% yield. A HEW coupling of **2**, 4-(2-hydroxyethoxy)-benzaldehyde,[62] gave distyrylbenzene **3** in 85% yield. Malonate **4** was obtained in 86% yield by esterification of malonyl dichloride from its distyryl alcohol **3**.

Methanofullerene **5**, whose structure and synthesis are reported in the ESI,† was used as a reference methanofullerene derivative lacking the distyrylbenzene moiety.

Linear absorption and emission

All the photophysical parameters obtained for dyad **1** and relative precursor model compounds are summarized in Table 1.

Steady-state UV-Vis absorption spectra of dyad **1** and model compounds **3–5** were recorded in air-saturated toluene solutions and reported in Fig. 1. The spectra of compounds **3** (triangles) and **4** (circles) show the characteristic features of DSB chromophores, with two principal maxima at 395 and 330 nm. The absorption spectrum of the dimeric form **4** is, within the experimental error, equivalent to twice the absorption spectrum of **3**, proving that no interaction takes place between the DSB moieties in the ground electronic state. The fullerene derivative **5** (squares) shows the absorption spectrum typical of functionalized methanofullerenes with the main band at 339 nm, which is broader with respect to pristine [60]fullerene, and an additional band at 433 nm.[66] The spectrum also displays a very weak absorption in the whole visible range extending up to 700 nm. (see ESI for a direct comparison of [60]fullerene and compound **5** spectra).† The absorption spectrum of dyad **1** (solid line, no symbols) discloses superimposed features of fullerene and DSB. From 450 to 380 nm the spectrum is dominated by the absorption of the DSB dimer **4**, while at shorter wavelength the contribution of the fullerene unit becomes noticeable. Within experimental error, the absorption spectrum of **1** matches the profile obtained by summation of the absorption spectra of the two individual moieties that constitute the dyad (dashed line) in the whole investigated spectral range, except for a slight deviation in the blue side. This deviation can originate from weak interactions between the two units or, more likely, is the result of errors associated with the absolute measure of the extinction coefficient, becoming more relevant in the blue side due to increasing scattering contributions. These results are in agreement with previous studies on donor–acceptor dyads in solution and suggest that there is no ground-state interaction between the fullerene and the DSB moieties. This is also confirmed by the presence of the weak but characteristic long wavelength absorption signal between 500 and 700 nm, as shown in the inset of Fig. 1. These bands are characteristic of the [60]fullerene derivatives and their presence in the absorption spectrum of **1** means that the π-conjugated structure of [60]fullerene and thus its photophysical properties, are not perturbed by functionalization with the DSB moiety.

The possible presence of energy or charge transfer processes occurring after excitation of **1** between the DSB and fullerene moieties can be ascertained through emission spectroscopy.

Fig. 2 shows the emission spectra of **1** and **4** in toluene after excitation of the samples at 400 nm in the same experimental conditions. The emission spectrum of **3** (not shown) presents the same features as **4**, but is characterized by an intensity approximately halved with respect to an equimolar solution of **4**, an evidence of negligible interactions between the two branches. The emission of dyad **1** can be qualitatively described as the sum of emissions from the DSB and fullerene components. In the 400–600 nm region, the emission spectrum is dominated by the appearance of two bands at 440 and 470 nm, with a shoulder at about 500 nm, typical of DSB units, whereas in

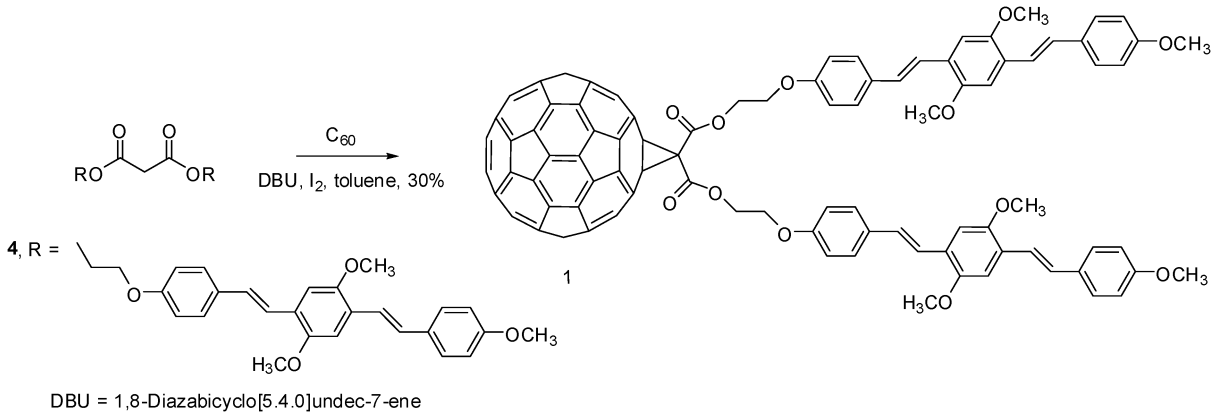

Scheme 1 Fullerene–distyrylbenzene conjugate **1** considered in this work.

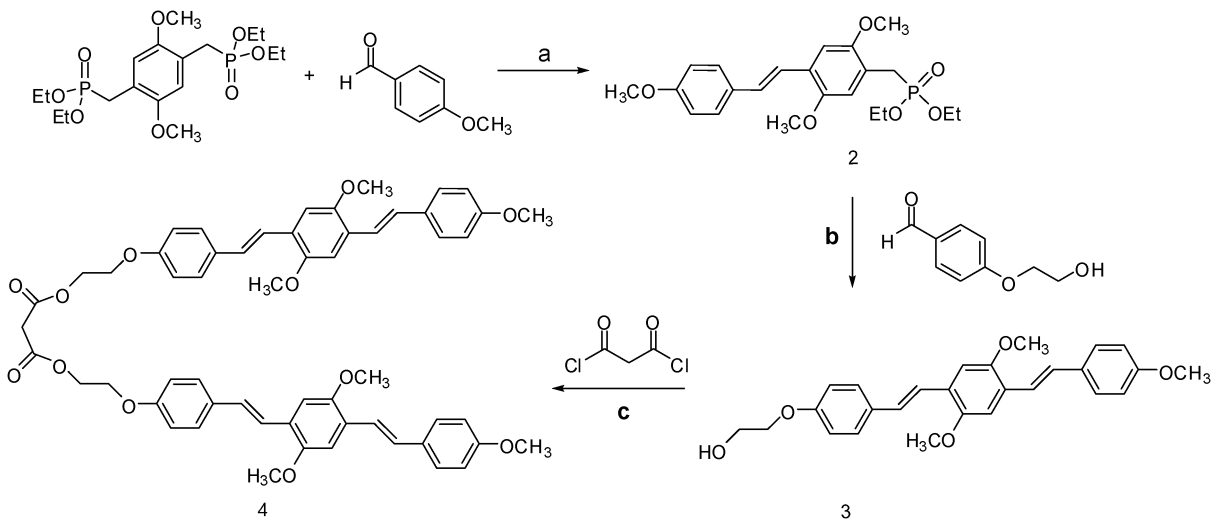

Scheme 2 Reagents and conditions: (a) *t*BuOK, DMF, 25 °C, 4 h, 62%; (b) *t*BuOK, DMF, 25 °C, 3 h, 85%; $NaHCO_3$, CH_2Cl_2, 25 °C, 15 h, 86%,

Table 1 Linear and nonlinear optical properties of compounds **1**, **3–5**

Compound	λ_{max} abs/nm	ε^a/M^{-1} cm^{-1}	λ_{max} fluo/nm	FQY^b	σ_{TPA} (GM) @ λ_{exc} = 740 nm
1	336 392 570	96 700 89 000 1000	440, 468, 500(shoulder), 705	0.008 ± 0.001	111 ± 10
3	333 397	18 300 40 700	442, 470, 500(shoulder)	0.96 ± 0.07	42 ± 6
4	333 395	48 300 85 600		0.70 ± 0.07	74 ± 6
5	339 429 570 (broad)	40 600 2400 1000	705	/	/

[a] Estimated error: 15%. [b] Calculated in the 400–600 nm interval.

the red side of the spectrum, between 600 and 800 nm, it shows the characteristic emission of fullerene cage at 705 nm (inset in Fig. 2). A much higher intensity of the bands at 440 and 470 nm with respect to that at 705 nm is indicative of the predominant contribution of DSB absorption at the excitation wavelength. The more important feature emerging from the comparison between the dyad and precursor compounds spectra is however the nearly complete quenching of DSB fluorescence in the dyad: there is more than two orders of magnitude decrease in fluorescence intensity relative to the free DSB **4**. In Fig. 2 the absolute fluorescence intensity of **1** was multiplied by 100 in order to be comparable with the fluorescence from **4** on

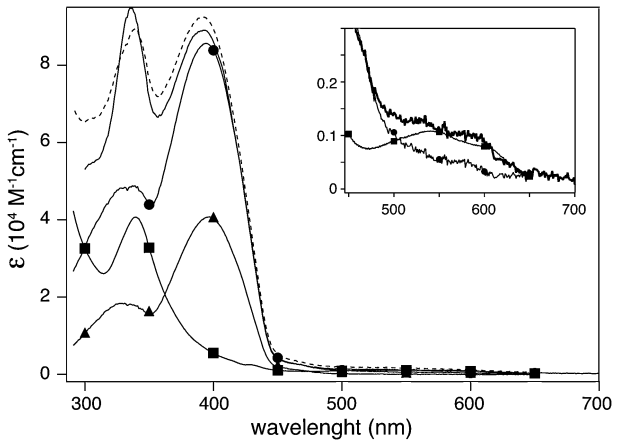

Fig. 1 Steady-state UV-Vis absorption spectra of **1** (no symbol) and model compounds **3** (triangles), **4** (circles), and **5** (squares) in air-saturated toluene. The dashed line is the profile obtained by summation of the absorption spectra of **4** and **5**.

the same intensity scale. The fluorescence spectra of compound **3** in toluene and of an equimolar solution of [60]fullerene and compound **3** are almost indistinguishable, whereas the fluorescence of an equimolar solution of **1** in toluene shows a dramatic change with respect to the previous two (see ESI).† These measurements confirm that at the concentrations investigated in this study, interactions between [60]fullerene and DSB occur only when they are covalently linked.

The quenching of the DSB emission in dyad **1** can be explained if either an energy or electron transfer process occurs from the excited DSB unit towards the fullerene, giving rise to an efficient non-radiative decay channel for the relaxation dynamics of **1**. In principle, the presence of energy transfer in fullerene dyads can be verified recording the fluorescence excitation spectrum for the fullerene emission, collected at 705 nm. However, the excitation profile obtained for **1** monitoring the 705 nm emission was too weak to give any useful information.

The amount of quenching was quantified by measuring the fluorescence quantum yields (FQY) of compounds **1**, **3** and **4**,

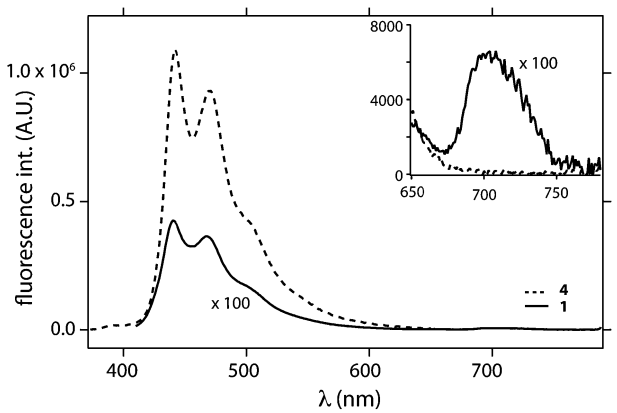

Fig. 2 Emission spectra of compounds **1** (solid line) and **4** (dashed line) recorded at λ_{ex} = 400 nm; the absolute fluorescence intensity for compound **1** has been scaled by 100 in order to compare the data on the same scale. The inset shows an enlargement of the red side of the spectra where the fullerene moiety emits.

excited at 330 nm, in the spectral region between 400 and 600 nm.[67]

Coumarin 153 (FQY = 0.56) and Coumarin 102 (FQY = 0.93) in ethanol, are used as standards.[68] The results are summarized in Table 1. The high FQY of **3** and **4** confirms that these compounds are extremely strong fluorophores, as already proven for differently functionalized DSB compounds.[69,70] On the other hand, the FQY of dyad **1** is less than 1%, supporting the presence of highly efficient non-radiative decay channels involving the fullerene unit.

Two photon absorption

The TPA properties of **1**, **3** and **4**, dissolved in toluene were investigated with the two photon induced fluorescence (TPIF) technique in the femtosecond regime. The TPA spectrum of **5** could not be determined since its fluorescence emission in the near-IR (680–800 nm) cannot be detected by our experimental-setup (detection window: 350–600 nm).

Absolute values of TPA cross section (σ_{TPA}) for a sample can be obtained comparing the TPIF emission of the sample with the emission of a standard molecule, whose σ_{TPA} and FQY are known:

$$\sigma_{TPA,s} = \frac{q_s C_r}{q_r C_s}\left(\frac{n_s}{n_r}\right)^2 \frac{\Phi_r}{\Phi_s}\sigma_{TPA,r} \qquad (1)$$

where $\sigma_{TPA,i}$ are the TPA cross sections, q_i are the coefficients of the quadratic fit of the TPIF intensity as a function of incident laser pulse energy, n_i the refractive indices, Φ_i the FQYs and C_i the concentrations of the sample ($i = s$) and the reference standard ($i = r$).

At room temperature, it is reasonable to assume that the fluorescence efficiency, from the lowest-lying singlet electronic state, does not change if this state is populated by one- or two-photon excitation, making it therefore possible to insert in eqn (1) the values of FQYs which were estimated with linear fluorescence experiments. The reference standard used is a solution of fluorescein in water (pH > 11), whose σ_{TPA} in the same spectral range is given in references 71 and 72. The FQY of the fluorescein standard is set equal to 0.90.[67]

In Fig. 3 the TPA spectra of **1** (squares), **3** (circles), and **4** (triangles) in toluene are compared with the respective normalized linear absorption spectra, also in toluene. The TPA data points are plotted against half the laser excitation wavelength, so that direct comparison with the one-photon absorption spectrum is easily accomplished. The error bars are estimated through an error propagation procedure. In particular, the error bar affecting the TPA data of **1** is larger than the one of **3** and **4**, since the relative error estimated for the FQY is 20 and 10%, respectively.

The TPA spectrum of **3** shows a steady increase of the TPA cross section as the wavelength decreases and no maximum is observed in the spectral range investigated. Molecule **3** is almost a symmetrical D-π-D structure, where D indicates the terminal electron-donor group, and π is a conjugated bridge. The general structure D-π-D is one of the most recurring designs for chromophores endowed with large σ_{TPA}. Experimental and theoretical evidence showed indeed that bis-donor substituted compounds could have σ_{TPA} values more than one

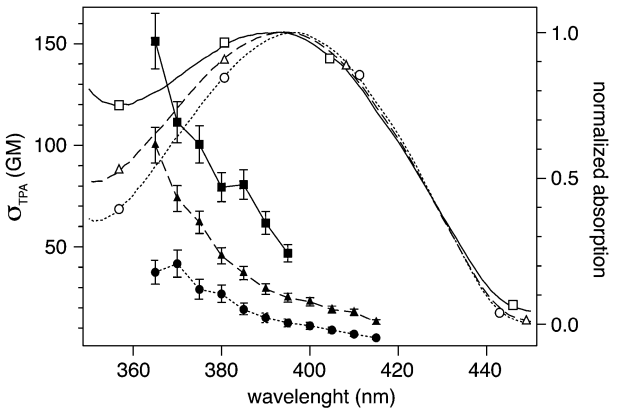

Fig. 3 Two-photon absorption spectra of compounds **1** (squares), **3** (circles), and **4** (triangles) in toluene. The corresponding normalized linear absorption spectra are also reported. The TPA data are plotted against half the excitation wavelength employed, in order to allow a direct comparison with the linear spectra.

order of magnitude larger than the corresponding pristine unsubstituted molecules. Theoretical studies allowed correlating this enhancement with intramolecular charge transfer from the terminal D groups to the π-bridge. Each modification of the molecular structure increasing the amount of intramolecular charge transfer can thus be exploited to synthesize molecules with larger σ_{TPA} absolute values. More specifically, it was found that σ_{TPA} increases when (i) the electron-donating character of the D group is strengthened, (ii) the conjugation length of the π-system is increased (since the charge is transferred over a longer distance) and (iii) when electron acceptors (A) are attached to the π bridge, to form the general structure D-π-A-π-D (wherein the amount of charge transferred is increased).[70,73]

Among D-π-D structures, functionalized DSB have received a lot of attention, in particular, when D at the terminus phenyl rings are N,N-dialkylamino groups.[69,70] For these structures, the maxima of the one- and two-photon absorption spectra do not coincide, and the TPA peak is shifted towards shorter wavelengths with respect to the one-photon maximum, as it also happens for **3**. The absolute value of the σ_{TPA} in these compounds (up to 1000 GM) is, however, one order of magnitude larger than that measured for DSB **3** (up to 50 GM) probably because of the weaker electron-donating capability of the alkyloxy groups in **3** in comparison with the aforementioned N,N-dialkyls. In our case the use of DSB **3** has been dictated mainly by the fact that the corresponding DSB with a N,N-dialkyl terminus is not stable under the conditions (DBU/I_2) employed for the cyclopropanation reaction to [60]fullerene.

The TPA spectrum of **4** follows the same wavelength dependence as **3** and its absolute value is about twice the TPA cross section of **3** in the whole range investigated. This experimental finding confirms what has already been observed in the linear absorption spectra: *i.e.* the two DSB units in **4** do not interact noticeably and therefore give two independent and additive contributions to the whole TPA cross section.

Although the FQY of compound **1** in toluene in the 400–650 nm range is less than 1%, its TPIF signal shows the quadratic dependence typical of a TPA process in the whole range of excitation wavelengths investigated, therefore it was possible to record its TPA spectrum. The comparison between the absolute values of σ_{TPA} measured for **1** and **4**, shows a slight enhancement of the TPA efficiency of the fullerene dyad with respect to the DSB model precursor **4**. A similar enhancement was observed in the σ_{TPA} values of different conjugated chromophores upon attaching a terminal fullerene, both in the ns and fs regime.[28,74,75] Considering that pristine fullerene displays negligible nonlinearities,[76,77] this effect cannot be explained invoking an additive contribution, but is more likely due to the electron withdrawing property of fullerene. The presence of an electron-accepting moiety like the fullerene gives to the dyad a partial D-π-A-π-D character, which guarantees a better TPA efficiency.

Singlet oxygen production

One-photon sensitization experiments. The quantum yield of one-photon sensitized $^1O_2$ formation (Φ^Δ) of compound **1** is estimated through measurements of the 1270 nm emission intensity of $^1O_2$ upon excitation at 403 nm. At this wavelength the absorption is mainly due to the DSB moiety. Toluene is used as solvent for sample **1** as well as for the reference compounds: [60]fullerene and *meso*-TPP. CS_2 solutions were also investigated for comparison. The concentration of all solutions was adjusted to obtain a linear absorbance of about 0.3 at 403 nm; this guarantees comparable excitation conditions for both the sample and the standards solutions. The standard molecules [60]fullerene and *meso*-TPP in toluene have Φ^Δ equal to 1.0 and 0.88 respectively.[44]

A number of control experiments were preliminarily performed in order to assign the recorded signal to $^1O_2$ luminescence emission. Specifically, singlet oxygen signals were not observed from sensitizer-free solvents (toluene or CS_2) and nor from the degassed sample. The lifetime of $^1O_2$ in the two different solvents was also checked coupling the InGaAs photodiodes with a preamplifier and an oscilloscope. The signal decay was always single exponential, and the values of the $^1O_2$ lifetime, roughly estimated by a monoexponential fit of the recorded decays, were consistent with those expected in the analyzed solvents. More specifically, a lifetime of about 30 μs was obtained upon irradiation of toluene solutions of the standards and compound **1**, whereas a longer lifetime of about 5 ms was estimated for CS_2 solutions, in good agreement with literature data.[78–80] The singlet oxygen lifetimes observed show no dependence on the laser pulse energy in the whole range investigated.

The detection apparatus (InGaAs photodiode and Lock In) used to determine Φ^Δ allows recording only an average signal and is not sensitive to the temporal decay of the $^1O_2$ emission. In order to check if steady state conditions are reached in all the photophysical steps involved in $^1O_2$ production, the measurements have been performed with 0.2, 0.5 and 1 kHz repetition rate. The ratio between the signals of the sample and the standard does not show any dependence on the repetition rate, confirming that steady state conditions are reached.

For both standards and for **1** the $^1O_2$ emission signal displays a linear dependence on both concentration and

incident power, as expected for a one-photon promoted process. The singlet oxygen quantum yield Φ^{Δ} is determined from the relative intensity of singlet oxygen luminescence, measured under identical conditions, by the relation:

$$\Phi_s^{\Delta} = \Phi_r^{\Delta} \cdot \frac{\beta_r S_s}{\beta_s S_r} \qquad (2)$$

where subscripts s and r refer to the sample and the standard, respectively. S_i ($i = s, r$) is the $^1O_2$ luminescence signal for the ith species and β_i is a correction factor accounting for the number of absorbed photon, that, in turn, depends on the absorbance of the solution at the wavelength of the incident laser beam (A_i) and on its intensity (I_0):

$$\beta_i = I_0(1 - 10^{-Ai}) \qquad (3)$$

The estimates for Φ^{Δ} gathered by comparison with [60]-fullerene and *meso*-TPP are 0.33 ± 0.08 and 0.44 ± 0.06, respectively. These values are considerably lower than the Φ^{Δ} of pristine fullerene.

The $^1O_2$ generation efficiency of [60]fullerene mixed with compound **3** in toluene does not show this reduction, and is similar to the one of [60]fullerene, within the experimental error (see ESI).† These measurements confirm that at the concentrations investigated in this study, the reduction in Φ^{Δ} occurs only when the two units are covalently linked.

The decrease in the efficiency of $^1O_2$ production by functionalized fullerenes with respect to pristine [60]fullerene is a well documented phenomenon, and has already been observed in different classes of adducts.[46,81–83]

A first explanation can be found in the correlation between photophysical properties and topology of the fullerene core. Studies of a series of methanofullerene[46,81] and epoxyfullerene[46] adducts with an increasing number of addends demonstrated that multiple functionalization results in the perturbation of the conjugation of the fullerene core and in an ensuing rise of the triplet states energy and abatement of triplet and singlet oxygen quantum yields. However, in the mono-adducts the topology effect can indeed account only for 10% decrease in the singlet oxygen generation efficiency.[81]

A second factor contributing to the Φ^{Δ} reduction could be the shielding effect exerted by the DSB branches toward the photoactive fullerene core. This effect was observed in dendritic tris(bipyridine) ruthenium chelates[84] and, more recently, in dendritic-fullerene derivatives.[83] In the case of fullerene adducts, this effect led to a decrease of oxygen diffusion rate regardless of the solvent nature, but only in polar solvents was the delayed singlet oxygen sensitization accompanied by an effective decrease of Φ^{Δ}. This result was attributed to the more compact structure assumed by the dendrimer in polar solvents, resulting in a less effective orbital overlap between the active [60]fullerene core and the oxygen.[83] Our steady-state measurements are not sensitive to the dynamic aspects of the $^1O_2$ generation, so it was not possible to verify if the presence of the two DSB branches cause a relevant decrement of the oxygen diffusion rate. On the other hand, the use of a non-polar solvent like toluene should guarantee a relatively open configuration and a minimization of the shielding effect.

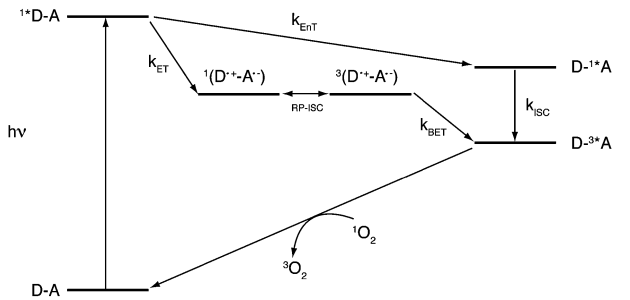

Fig. 4 Two possible mechanisms for singlet oxygen generation by dyad **1** in toluene. A represents the C_{60} core and D the DSB moiety. EnT = energy transfer; ET = electron transfer; BET = back electron transfer; ISC = intersystem crossing; RP-ISC = radical pair intersystem crossing. The energy levels $^1(D^{\bullet+}-A^{\bullet-})$ and $^3(D^{\bullet+}-A^{\bullet-})$ were drawn with energy intermediate between D−^{1}*A and ^{3}*D−A, in analogy with previous studies on porphyrin–fullerene dyads also in toluene (see ref. 82 and 87).

Having ruled out the topologic and the shielding effect as the primary cause of Φ^{Δ} reduction, the most plausible explanation is assuming the presence of competitive decay pathways. The mechanism most frequently invoked to describe the generation of singlet oxygen by photoexcited fullerene adducts (Fig. 4) involves preliminary photoexcitation of the chromophoric groups attached to the fullerene core (^{1}*D−C_{60}) followed by energy transfer to the [60]fullerene moiety (D−^{1}*C_{60}). The resulting singlet excited state of [60]fullerene is then readily converted to the long-lived triplet excited state (D−^{3}*C_{60}) *via* intersystem crossing. The final step is the energy transfer to molecular oxygen.

It was demonstrated that for pristine fullerene and simple fullerene derivatives, both intersystem crossing and energy transfer to molecular oxygen occur with nearly unitary quantum efficiency.[85,86] This means that the Φ^{Δ} reduction is most probably due to a less operative singlet energy transfer between the two moieties forming the dyad.

Another possible mechanism, recently proposed for porphyrin–fullerene dyads in toluene, is based on the results obtained with time-resolved electron paramagnetic resonance (TR-EPR) measurements.[82,87] This alternative mechanism (Fig. 4) involves electron transfer, intersystem crossing between radical pair species and back electron transfer to generate the fullerene triplet state (D−^{3}*C_{60}). The activation of such a mechanism could explain the loss of efficiency in the $^1O_2$ generation, as well as the small amount of energy transfer from DSB to fullerene detected by the fluorescence excitation measurements.

The involvement of a radical species in the sensitization mechanism can be indirectly verified checking the efficiency of $^1O_2$ generation in more polar solvents, capable of stabilizing radicalic intermediates. Comparison between the efficiency of $^1O_2$ sensitization in different solvents of pristine [60]fullerene with the one of dyad **1** shows a net decrease for the latter with respect to [60]fullerene, when the dielectric constant of the solvent increases. The solvents employed are toluene, chlorobenzene and benzonitrile, characterized by a sizable change of their dielectric constant (from 2.38 of toluene to 25.20 of benzonitrile). These experimental findings are an indirect confirmation of the involvement of charge separated species

in the proposed decay mechanism (details on the measurements are given in the ESI).†

Although corroborated by this indirect evidence, the presence of this pathway leading to formation of $D-^3*C_{60}$ from radical pair species could be confirmed eventually through TR-EPR measurements.

As a final remark it is important to point out that although the Φ^{Δ} of **1** is smaller than the Φ^{Δ} of [60]fullerene, it still reaches a 30% value, necessary for a molecule to be considered as a suitable candidate for photodynamic therapy. Furthermore **1** absorbs strongly in the visible, where most lasers actually employed in photodynamic therapy emit, whereas [60]fullerene shows just a vanishingly small absorption coefficient in this spectral range.

Two-photon sensitization experiments. It is reasonable to assume that irrespective of whether excitation is promoted by a one- or a two-photon process, fast relaxation to the lowest singlet excited S_1 state will take place. Since the process leading to singlet oxygen sensitization originates from S_1, the photophysics of $^1O_2$ will be independent of the excitation scheme. The main difference between the one-photon and the two-photon excitation schemes is the yield of S_1 population, being about 7-8 orders of magnitude lower for the two-photon process than for the one-photon process.[57] Thus, to be able to detect $^1O_2$ signal promoted by TPA, the molecule not only must efficiently produce singlet oxygen, but also have an appreciable TPA cross section.

The first attempt to detect $^1O_2$ luminescence was made irradiating a toluene solution of **4** at 806 nm. No signal could be detected within the noise level. This was partly expected since the TPA cross section of **1** at 806 nm is less than 50 GM (Fig. 3), too low to effectively populate the S_1 state with the available laser intensity.

In the light of the TPA measurements presented in Fig. 3, the experiment was repeated exciting at shorter wavelengths (710 and 750 nm), where the TPA cross section is large enough to generate a non negligible S_1 population. At these wavelengths the signal was dominated by a large contribution of scattered IR light, generated by the OPA800C, and not adequately removed with long-pass filters. It was however possible to discriminate between the scattered light and the $^1O_2$ luminescence emission comparing the signal recorded for the air-equilibrated and the degassed solution (Fig. 5a). The signal recorded from the degassed tube arises only from scattering processes, and shows indeed the typical linear dependence on the pulse energy. Generation of $^1O_2$ by one-photon processes can be ruled out because the absorbance of the sample solution at these wavelengths is <0.002. On the other hand, the signal from the air-equilibrated solution shows a super-linear dependence on the pulse energy, as expected for multi-photon processes. After correction of the air-equilibrated solution signal for the scattered light, a clear quadratic dependence is found (Fig. 5b, 6). Since for TPA, the $^1O_2$ intensity is known to be proportional to the square of laser intensity, we can ascribe these signals to sensitization of singlet oxygen promoted by two-photon excitation.

Fig. 6 shows the double logarithmic plot of $^1O_2$ intensity against laser pulse energy at 710 and 750 nm excitation. The figure indicates that the $^1O_2$ data recorded upon 710 and 750 nm irradiation are consistent with a two-photon absorption scheme. The linear slopes generated by a least-squares analysis are 1.9 ± 0.1 and 1.8 ± 0.15 for 710 and 750 nm excitation, respectively, as expected for a TPA process. The data obtained with 403 nm excitation (slope 1.01 ± 0.05) are also reported for comparison.

As a control experiment, we also irradiated in the same conditions sensitizer-free toluene and solutions of the two standards ([60]fullerene and *meso*-TPP) in toluene, both air-equilibrated and degassed. In all cases, no signal with quadratic dependence was recorded and after correction for scattered light, the signal resulted in zero.

Experimental

Materials

[60]fullerene was purchased from Bucky USA (99.5%). 2,5-bis(diethylphosphonate)-1,4-dimethoxybenzene,[61] 4-(2-hydroxy-ethoxy)-benzaldehyde[62] and methanofullerene **5** (Fig. S13, ESI)† were prepared as previously reported. All other reagents were used as purchased from Sigma-Aldrich. The toluene for photophysical characterizations of derivatives **1–5** was a commercial spectrophotometric-grade solvent used without further purification. Thin layer (TLC) and column chromatography were performed using a Polygram SilG/UV254 (TLC plates) and silica gel MN 60 (70–230 Mesh) by Macherey-Nagel.

Instrumentation

^1H (250.1 MHz) and ^{13}C (62.9 MHz) NMR spectra were recorded on a Bruker AC-F 250 spectrometer. IR spectra were recorded on a Perkin-Elmer FT-IR model 1720X. Oily compounds were measured between KBr windows; powders were measured making KBr pellets. HPLC analysis of **1** was carried out on a Shimadzu LC-8A instrument, equipped with a Shimadzu UV6000LP photodiode array detector by Thermo Scientific, using a SiO_2 Phenomenex Luna column (150 × 4.6 mm, 4 μm, eluent: toluene, flow rate: 2 ml min^{-1}). ESI-MS spectra were recorded on a LC-MSD-Trap-SL (Agilent Technologies, Palo Alto – USA). Samples were dissolved in methanol ($\sim 10^{-5}$ M) and injected in a stream of the same solvent at 50 μl min^{-1} (nitrogen nebulizing gas pressure = 20 psi; flow = 5 L min^{-1}; T = 325 °C). APPI-MS spectrum of derivative **1** was recorded on the same instrument (nitrogen nebulizing gas pressure = 30 psi; flow = 4 L min^{-1}; T = 325 °C; vaporizer T = 350 °C). The sample, dissolved in cyclohexane ($\sim 10^{-5}$ M), was directly infused in the APPI source through a syringe pump (100 μl min^{-1}).

Absorption and fluorescence spectra of all compounds were carried out with a Cary 5 (Varian) and a Fluoromax (Spex Jobin-Yvon), respectively. Typical concentrations were $\sim 1 \times 10^{-5}$ M for one-photon absorption and 1×10^{-6} M for emission measurements. The TPA experiments (on samples $\sim 1 \times 10^{-4}$ M) were performed using the TPA induced fluorescence technique (TPIF). The technique and the experimental set-up were described in detail elsewhere.[63] Briefly, a tunable Ti:Sapphire femtosecond laser system (Coherent Mira Optima 900-F), delivering pulses with approximately 130 fs

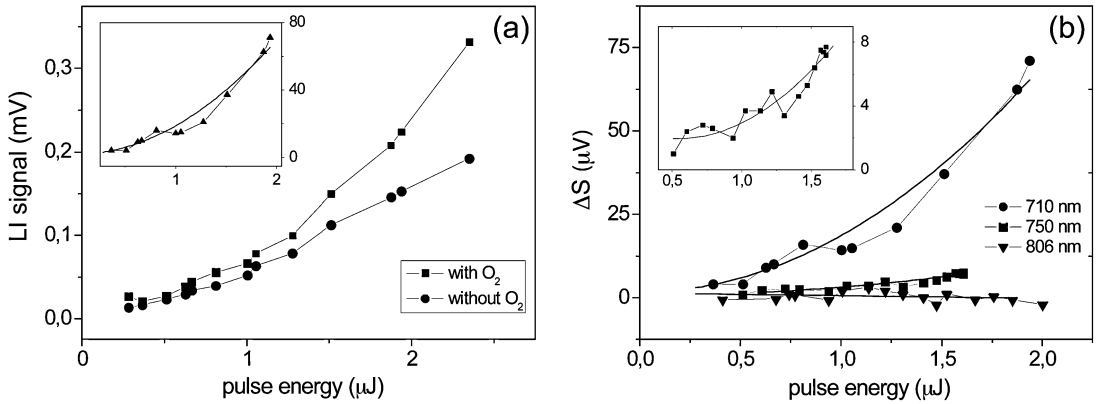

Fig. 5 (a) Comparison between the signals recorded for an air-equilibrated (squares) and a degassed (circles) solution of **1** in toluene. The signal recorded in the degassed solution is only due to scattering, not completely removed, as indeed proven by the typical linear dependence on the pulse energy. In the inset the actual signal due to $^1O_2$ luminescence emission obtain after subtraction of the scatter. (b) TPA promoted $^1O_2$ generation at different wavelengths. The signals were already corrected for the scatter contribution. The inset shows an enlargement of the data at 750 nm.

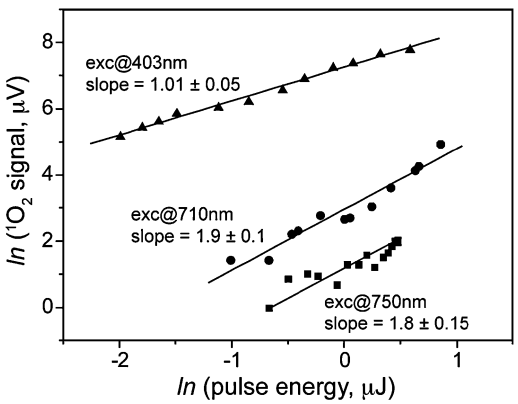

Fig. 6 Double logarithmic plot of $^1O_2$ intensity against pulse energy on air-equilibrated toluene solutions of **1** at 403 nm (triangles), 710 nm (circles) and 750 nm (squares) excitation. Dots are experimental data and the solid lines are linear fits. The signals were corrected for the scatter contribution using a degassed solution of the sample.

duration at the repetition rate of 76 MHz is used to excite the sample from 730 to 830 nm. The laser pulses are focalized by a 40 cm lens inside a 1 cm path cuvette, so that the Rayleigh range extends almost over the whole depth of the cuvette. The fluorescence signal, collected at 90° by a 4 cm lens, is measured with a photomultiplier tube and recorded by a computer-controlled digital oscilloscope as a function of input beam intensity. The quadratic dependence of the fluorescence signal with respect to the incident laser intensity was verified at each excitation wavelength.

The one-photon and two-photon $^1O_2$ generation performances were investigated through direct measurement of the dye-sensitized singlet oxygen luminescence at 1270 nm. In the one-photon experiment, the sample was excited at 403 nm by the frequency-doubled emission of a Ti-sapphire amplified laser system (Spectra Physics) characterized by 150 fs long pulses at several repetition rates in the range 0.2–1 kHz. The laser pulses were suitably attenuated by neutral density filters as well as a combination of a half-waveplate and a polarizer. The sample solution was held in a 4 mm diameter quartz tube to open air, and no oxygen was added. Quartz tubes are used, instead of fluorescence cuvettes, because they allow degassing and sealing the sample under vacuum after several freeze-pump-thaw cycles. This procedure was applied to all the solutions employed, to check that the signal recorded by the experimental set-up is generated exclusively by $^1O_2$ emission at 1270 nm. The one-photon excited emission was collected by a combination of lenses at 90° with respect to the excitation pulses, and sent to a room temperature InGaAs photodiode (Hamamatsu). The signal from the photodiode was then averaged by a Lock-In amplifier and recorded by a computer. The two-photon promoted $^1O_2$ generation was measured at three different wavelengths: 710, 750 and 806 nm. The fundamental emission of the laser at 806 nm was employed directly or used to pump an optical parametric amplifier (OPA800C-Spectra Physics) set to deliver pulses at 710 and 750 nm. A slightly different acquisition geometry was employed at these wavelengths: luminescence was detected directly from the front face of the sample by a liquid-nitrogen cooled InGaAs photodiode/preamplifier (EG&G Judson) system. An interference filter centred at 1270 ± 20 nm (CVI) was placed directly in front of the photodiodes to discriminate the singlet oxygen emission from the laser scattered light and all other sample emissions.

Syntheses and selected analytical data: methanofullerene 1

To a solution of [60]fullerene (77 mg, 0.11 mmol, 1.2 eq.), malonate **4** (83 mg, 0.09 mmol, 1 eq.) and iodine (27 mg, 0.11 mmol, 1.2 eq) in toluene (60 ml), a solution of DBU (20 mg, 0.13 mmol, 1.2 eq) in 10 ml toluene was added dropwise under a nitrogen atmosphere over a period of 10 min. When the addition was complete, the brownish mixture was stirred for 2 h at rt. The solvent was removed under reduced pressure and the crude product purified by flash chromatography (SiO_2, eluent: toluene, then toluene/ethyl acetate 95:5). The fractions containing the product were concentrated to a small volume under reduced pressure and were transferred into a centrifuge tube. The product was precipitated from cyclohexane and washed with methanol. 43.5 mg (30%) of **1** were isolated as a brownish powder. ^{1}H-NMR (250 MHz, $CDCl_3$, 25 °C, TMS) δ 7.49–7.42 (t, 8H), 7.37–6.98 (m, 8H), 7.08 (s, 4H),

6.90–6.89 (d, 4H), 6.87–6.85 (d, 4H), 4.82–4.80 (t, 4H), 4.34–4.32 (t, 4H), 3.89 (s, 12H), 3.83 (s, 6H). ^{13}C-NMR (250 MHz, CS_2CDCl_3 4:1, 25 °C, TMS) δ 163.05, 159.18, 157.78, 151.32, 151.27, 145.30, 145.19, 145.13, 145.04, 144.91, 144.70, 144.65, 143.90, 143.06, 143.03, 142.26, 141.85, 140.98, 139.15, 131.59, 130.78, 129.11, 128.30, 128.00, 127.86, 126.72, 126.33, 121.86, 121.25, 114.83, 114.19, 108.75, 108.63, 71.32, 65.60, 65.38, 56.02, 55.12, 51.76. HPLC: R_f (**1**) = 3.38 min; purity >98%. APPI-MS m/z 1651 $[M+H]^+$.

Phosphonate 2

To a solution of 2,5-bis(diethylphosphonate)-1,4-dimethoxybenzene (10.0 g, 22 mmol) and 4-methoxybenzaldehyde (3.10 g, 22 mmol) in 200 ml of DMF, a solution of *t*BuOK (1.72 g, 15 mmol) in 15 ml of DMF was added dropwise, under a nitrogen atmosphere, over a period of 1 h. When the addition was complete, the mixture was stirred at room temperature for 3 h and then concentrated at reduced pressure. The crude product was purified by unreacted aldehyde and symmetrical distyrylbenzene by flash chromatography (SiO_2, eluent: ethyl acetate/petroleum ether 8:2, then ethyl acetate/ethanol 9:1). 5.74 g (62%) of phosphonate **2** were isolated as a light yellow oil that solidifies on standing. ^{1}H-NMR (250 MHz, $CDCl_3$, 25 °C, TMS) δ 7.49–7.46 (d, 2H), 7.35–7.00 (q, 2H), 7.08 (s, 1H), 6.94–6.92 (d, 1H), 6.91–6.87 (d, 2H), 4.11–3.99 (m, 4H), 3.87 (s, 3H), 3.85 (s, 3H), 3.82 (s, 3H), 3.30–3.21 (d, 2H), 1.29–1.23 (t, 6H). ^{13}C-NMR (250 MHz, $CDCl_3$, 25 °C, TMS) δ 159.20, 151.15, 130.51, 128.24, 127.62, 125.87, 121.05, 119.85, 114.49, 113.94, 108.29, 61.89, 56.12, 55.18, 27.67, 25.45, 16.27. IR(KBr) $\nu\sim$ 2983, 2905, 2838, 1603, 1514, 1413, 1265, 1222, 1036, 971, 818 817 cm^{-1}. ESI-MS: m/z 421 $[M+H]^+$.

Distyrylbenzene 3

To a solution of 4-(2-hydroxyethoxy)-benzaldehyde (0.59 g, 3.56 mmol) and phosphonate **2** (1.50 g, 3.56 mmol) in 20 ml DMF, a solution of *t*BuOK (1.72 g, 8.82 mmol) in 10 ml of DMF was added dropwise under a nitrogen atmosphere over a period of 1 h. When the addition was complete, the mixture was stirred at room temperature for 2 h and then concentrated at reduced pressure. The crude product was dissolved in CH_2Cl_2 and washed with dil. HCl. The organic phase, dried over Na_2SO_4, was concentrated and the residue crystallized from CH_2Cl_2/hexane. 1.30 g (85%) of **3** were isolated as yellow crystals. ^{1}H-NMR (250 MHz, $CDCl_3$, 25 °C, TMS) δ 7.50–7.47 (d, 4H), 7.39–7.00 (q, 4H), 7.11 (s, 2H), 6.93–6.91 (d, 2H), 6.89–6.88 (d, 2H), 4.11–4.09 (t, 2H), 3.99–3.95 (t, 2H), 3.91 (s, 6H), 3.83 (s, 3H). ^{13}C-NMR (250 MHz, $CDCl_3$, 25 °C, TMS) δ 159.18, 158.17, 151.33, 131.16, 130.68, 128.34, 128.14, 127.78, 126.58, 126.39, 121.39, 121.10, 114.70, 114.06, 108.90, 69.20, 61.47, 56.35, 55.30. IR(KBr) ν ~ 3033, 2996, 2936, 2832, 1601, 1510, 1406, 1249, 1209, 1175, 1041, 963, 847, 819 cm^{-1}. ESI-MS: m/z 432 $[M]^+$.

Distyryl malonate 4

To a solution of distyrylbenzene **3** (0.1 g, 0.23 mmol, 2 eq.) in 10 ml of anhydrous CH_2Cl_2, $NaHCO_3$ (77.4 mg, 0.92 mmol, 8 eq) was added under a nitrogen atmosphere. After 30 min at room temperature, a solution of malonyl dichloride (16.3 mg, 0.12 mmol, 1 eq) in 5 ml of dry CH_2Cl_2 was slowly added dropwise over a period of 2 h. The mixture was left stirring for additional 12 h at room temperature, then the solvent was removed under reduced pressure. The crude product was purified by flash chromatography (SiO_2, eluent: ethyl acetate/petroleum ether 7:3). 92.6 mg (86%) of derivative **4** were isolated after crystallization from a THF/ethanol mixture. ^{1}H-NMR (250 MHz, $CDCl_3$, 25 °C, TMS) δ 7.50–7.45 (q, 8H), 7.37–7.02 (q, 8H), 7.09 (s, 4H), 6.91–6.88 (d, 4H), 6.87–6.85 (d, 4H), 4.52–4.48 (t, 4H), 4.19–4.16 (t, 4H), 3.90 (s, 12H), 3.83 (s, 6H), 3.50 (s, 2H). IR(KBr) $\nu\sim$ 3035, 2998, 2932, 2832, 1754, 1733, 1603, 1510, 1406, 1247, 1208, 1174, 1039, 965, 848, 817 cm^{-1}. ESI-MS: m/z 932 $[M]^+$.

Conclusion

In the search for novel materials acting as photosensitizers for two-photon excited photodynamic therapy, we synthesized and characterized a prototype fullerene dyad in which pristine [60]fullerene was functionalized with distyrylbenzene moieties. The use of a two-photon absorption excitation process as an alternative to one-photon processes in PDT treatment is advantageous because of the possibility to focus on a confined and small treatment area of diseased tissues with a greater depth and at the same time avoid damage to healthy surrounding tissues. The success of this approach relies on the availability of water–soluble molecules with significantly large TPA cross-section and singlet oxygen generation. The dyad proposed in this work represents a promising prototype system in which the high efficiency of [60]fullerene as singlet oxygen sensitizer is exploited in combination with the high TPA cross section of distyrylbenzene moieties.

The photophysical properties of the dyad were preliminarily characterized by linear and nonlinear optical experiments and compared with the properties of model precursor compounds. Linear fluorescence experiments highlighted the presence of strong quenching of the DSB emission and confirmed the presence of energy or electron transfer processes from the excited DSB unit towards the fullerene. Moreover, TPA measurements showed a two-fold enhancement of the TPA cross-section in the dyad with respect to the DSB model compound.

Characterization of singlet oxygen sensitization showed that, although the quantum yield of the dyad is smaller than the one of the pristine [60]fullerene, it still reaches a 30% value, necessary for a molecule to be considered a suitable candidate for photodynamic therapy. More interestingly, it was possible to record sensitization of singlet oxygen promoted also by two-photon excitation.

The approach utilized in this study provided a reliable starting point for the design of efficient [60]fullerene-based structures exploitable in two-photon excited PDT.

Acknowledgements

Financial support was provided by the grants: FIRB RBNE033KMA and PRIN 2007LN873M (MIUR), PROMO (CNR-INSTM), CPDA074184 (Univ. of Padova) and MISCHA (Fondazione CARIPARO). We wish to thank Dr E. Marotta, Univ. of Padova for APPI-MS measurements.

References

1 G. Dennler, M. C. Scharber and C. J. Brabec, *Adv. Mater.*, 2009, **21**, 1323–1338.
2 H. Imahori, Y. Mori and Y. Matano, *J. Photochem. Photobiol., C*, 2003, **4**, 51–83.
3 J. Roncali, *Chem. Soc. Rev.*, 2005, **34**, 483–495.
4 B. C. Thompson and J. M. J. Frechet, *Angew. Chem., Int. Ed.*, 2008, **47**, 58–77.
5 D. Gust, T. A. Moore and A. L. Moore, *Acc. Chem. Res.*, 2001, **34**, 40–48.
6 G. Brusatin and R. Signorini, *J. Mater. Chem.*, 2002, **12**, 1964–1977.
7 R. Signorini, M. Meneghetti, R. Bozio, M. Maggini, G. Scorrano, M. Prato, G. Brusatin, P. Innocenzi and M. Guglielmi, *Carbon*, 2000, **38**, 1653–1662.
8 V. P. Belousov, I. M. Belousova, V. P. Budtov, V. V. Danilov, O. B. Danilov, A. G. Kalintsev and A. A. Mak, *J. Opt. Techn.*, 1997, **64**, 1081–1109.
9 D. M. Guldi, *Chem. Soc. Rev.*, 2002, **31**, 22–36.
10 F. Diederich and C. Thilgen, *Science*, 1996, **271**, 317–323.
11 M. Prato and M. Maggini, *Acc. Chem. Res.*, 1998, **31**, 519–526.
12 A. Hirsch, *Top. Curr. Chem.*, 1999, **199**, 1–65.
13 P. A. Liddell, G. Kodis, A. L. Moore, T. A. Moore and D. Gust, *J. Am. Chem. Soc.*, 2002, **124**, 7668–7669.
14 P. A. Liddell, D. Kuciauskas, J. P. Sumida, B. Nash, D. Nguyen, A. L. Moore, T. A. Moore and D. Gust, *J. Am. Chem. Soc.*, 1997, **119**, 1400–1405.
15 H. Imahori, D. M. Guldi, K. Tamaki, Y. Yoshida, C. P. Luo, Y. Sakata and S. Fukuzumi, *J. Am. Chem. Soc.*, 2001, **123**, 6617–6628.
16 H. Imahori, K. Tamaki, Y. Araki, Y. Sekiguchi, O. Ito, Y. Sakata and S. Fukuzumi, *J. Am. Chem. Soc.*, 2002, **124**, 5165–5174.
17 H. Imahori, K. Tamaki, D. M. Guldi, C. P. Luo, M. Fujitsuka, O. Ito, Y. Sakata and S. Fukuzumi, *J. Am. Chem. Soc.*, 2001, **123**, 2607–2617.
18 H. Imahori, K. Yamada, M. Hasegawa, S. Taniguchi, T. Okada and Y. Sakata, *Angew. Chem., Int. Ed. Engl.*, 1997, **36**, 2626–2629.
19 C. Luo, D. M. Guldi, H. Imahori, K. Tamaki and K. Sakata, *J. Am. Chem. Soc.*, 2000, **122**, 6535–6551.
20 M. A. Herranz, B. Illescas, N. Martin, C. P. Luo and D. M. Guldi, *J. Org. Chem.*, 2000, **65**, 5728–5738.
21 N. Martin, L. Sanchez and D. M. Guldi, *Chem. Commun.*, 2000, 113–114.
22 N. Martin, L. Sanchez, M. A. Herranz and D. M. Guldi, *J. Phys. Chem. A*, 2000, **104**, 4648–4657.
23 L. Sanchez, I. Perez, N. Martin and D. M. Guldi, *Chem.–Eur. J.*, 2003, **9**, 2457–2468.
24 D. M. Guldi, M. Maggini, G. Scorrano and M. Prato, *J. Am. Chem. Soc.*, 1997, **119**, 974–980.
25 M. Fujitsuka, N. Tsuboya, R. Hamasaki, M. Ito, S. Onodera, O. Ito and Y. Yamamoto, *J. Phys. Chem. A*, 2003, **107**, 1452–1458.
26 A. S. D. Sandanayaka, K. Matsukawa, T. Ishi-i, S. Mataka, Y. Araki and O. Ito, *J. Phys. Chem. B*, 2004, **108**, 19995–20004.
27 H. P. Zeng, T. T. Wang, A. S. D. Sandanayaka, Y. Araki and O. Ito, *J. Phys. Chem. A*, 2005, **109**, 4713–4720.
28 L. Y. Chiang, P. A. Padmawar, T. Canteenwala, L. S. Tan, G. S. He, R. Kannan, R. Vaia, T. C. Lin, Q. D. Zheng and P. N. Prasad, *Chem. Commun.*, 2002, 1854–1855.
29 H. I. Elim, R. Anandakathir, R. Jakubiak, L. Y. Chiang, W. Ji and L. S. Tan, *J. Mater. Chem.*, 2007, **17**, 1826–1838.
30 H. I. Elim, S. H. Jeon, S. Verma, W. Ji, L. S. Tan, A. Urbas and L. Y. Chiang, *J. Phys. Chem. B*, 2008, **112**, 9561–9564.
31 N. Camaioni, G. Fabbrini, E. Menna, M. Maggini, G. Ridolfi and A. Zanelli, *New J. Chem.*, 2006, **30**, 335–342.
32 J. F. Eckert, J. F. Nicoud, J. F. Nierengarten, S. G. Liu, L. Echegoyen, F. Barigelletti, N. Armaroli, L. Ouali, V. Krasnikov and G. Hadziioannou, *J. Am. Chem. Soc.*, 2000, **122**, 7467–7479.
33 J. F. Nierengarten, N. Armaroli, G. Accorsi, Y. Rio and J. F. Eckert, *Chem.–Eur. J.*, 2003, **9**, 36–41.
34 E. Peeters, P. A. van Hal, J. Knol, C. J. Brabec, N. S. Sariciftci, J. C. Hummelen and R. A. J. Janssen, *J. Phys. Chem. B*, 2000, **104**, 10174–10190.
35 D. M. Guldi and M. Prato, *Acc. Chem. Res.*, 2000, **33**, 695–703.
36 E. Nakamura and H. Isobe, *Acc. Chem. Res.*, 2003, **36**, 807–815.
37 Z. I. Yoshida, H. Takekuma, S. I. Takekuma and Y. Matsubara, *Angew. Chem., Int. Ed. Engl.*, 1994, **33**, 1597–1599.
38 S. D. M. Islam, M. Fujitsuka, O. Ito, A. Ikeda, T. Hatano and S. Shinkai, *Chem. Lett.*, 2000, 78–79.
39 A. Buvari-Barcza, J. Rohonczy, N. Rozlosnik, T. Gilanyi, B. Szabo, G. Lovas, T. Braun, J. Samu and L. Barcza, *J. Chem. Soc., Perkin Trans. 2*, 2001, 191–196.
40 T. M. Figueira-Duarte, J. Clifford, V. Amendola, A. Gegout, J. Olivier, F. Cardinal, M. Meneghetti, N. Armaroli and J. F. Nierengarten, *Chem. Commun.*, 2006, 2054–2056.
41 M. Triesscheijn, P. Baas, J. H. M. Schellens and F. A. Stewart, *Oncologist*, 2006, **11**, 1034–1044.
42 S. B. Brown and K. J. Mellish, *Expert Opin. Pharmacother.*, 2001, **2**, 351.
43 P. Babilas, S. Karrer, A. Sidoroff, M. Landthaler and R. M. Szeimies, *Photodermatol., Photoimmunol. Photomed.*, 2005, **21**, 142–149.
44 F. Wilkinson, W. P. Helman and A. B. Ross, *J. Phys. Chem. Ref. Data*, 1993, **22**, 113–262.
45 J. L. Anderson, Y. Z. An, Y. Rubin and C. S. Foote, *J. Am. Chem. Soc.*, 1994, **116**, 9763–9764.
46 T. Hamano, K. Okuda, T. Mashino, M. Hirobe, K. Arakane, A. Ryu, S. Mashiko and T. Nagano, *Chem. Commun.*, 1997, 21–22.
47 Y. Yamakoshi, N. Umezawa, A. Ryu, K. Arakane, N. Miyata, Y. Goda, T. Masumizu and T. Nagano, *J. Am. Chem. Soc.*, 2003, **125**, 12803–12809.
48 M. Ochsner, *J. Photochem. Photobiol., B*, 1997, **39**, 1–18.
49 C. S. Foote, *Photochem. Photobiol.*, 1991, **54**, 659–659.
50 Y. Liu, Y. L. Zhao, Y. Chen, P. Liang and L. Li, *Tetrahedron Lett.*, 2005, **46**, 2507–2511.
51 J. Hirayama, H. Abe, N. Kamo, T. Shinbo, Y. Ohnishi-Yamada, S. Kurosawa, K. Ikebuchi and S. Sekiguchi, *Biol. Pharm. Bull.*, 1999, **22**, 1106–1109.
52 J. P. Kamat, T. P. A. Devasagayam, K. I. Priyadarsini and H. Mohan, *Toxicology*, 2000, **155**, 55–61.
53 Y. Tabata, Y. Murakami and Y. Ikada, *Jpn. J. Cancer Res.*, 1997, **88**, 1108–1116.
54 W. R. Zipfel, R. M. Williams and W. W. Webb, *Nat. Biotechnol.*, 2003, **21**, 1369–1376.
55 M. D. Cahalan, I. Parker, S. H. Wei and M. J. Miller, *Nat. Rev. Immunol.*, 2002, **2**, 872–880.
56 J. Arnbjerg, M. Johnsen, P. K. Frederiksen, S. E. Braslavsky and P. R. Ogilby, *J. Phys. Chem. A*, 2006, **110**, 7375–7385.
57 P. K. Frederiksen, M. Jorgensen and P. R. Ogilby, *J. Am. Chem. Soc.*, 2001, **123**, 1215–1221.
58 M. Drobizhev, Y. Stepanenko, Y. Dzenis, A. Karotki, A. Rebane, P. N. Taylor and H. L. Anderson, *J. Phys. Chem. B*, 2005, **109**, 7223–7236.
59 J. R. Starkey, A. K. Rebane, M. A. Drobizhev, F. Q. Meng, A. J. Gong, A. Elliott, K. McInnerney and C. W. Spangler, *Clin. Cancer Res.*, 2008, **14**, 6564–6573.
60 H. A. Collins, M. Khurana, E. H. Moriyama, A. Mariampillai, E. Dahlstedt, M. Balaz, M. K. Kuimova, M. Drobizhev, V. X. D. Yang, D. Phillips, A. Rebane, B. C. Wilson and H. L. Anderson, *Nat. Photonics*, 2008, **2**, 420–424.
61 I. Brehm, S. Hinneschiedt and H. Meier, *Eur. J. Org. Chem.*, 2002, 3162–3170.
62 P. C. M. Mao, J. F. Mouscadet, H. Leh, C. Auclair and L. Y. Hsu, *Chem. Pharm. Bull.*, 2002, **50**, 1634–1637.
63 R. Signorini, C. Ferrante, D. Pedron, M. Zerbetto, E. Cecchetto, M. Slaviero, I. Fortunati, E. Collini, R. Bozio, A. Abbotto, L. Beverina and G. A. Pagani, *J. Phys. Chem. A*, 2008, **112**, 4224–4234.
64 A. Hirsch and M. Brettreich, *Fullerenes: Chemistry and Reactions*, Wiley-VCH, Weinheim, 2005.
65 H. Günther, *NMR Spectroscopy. An Introduction*, J. Wiley and Sons, Chichester, 1980.
66 R. V. Bensasson, E. Bienvenue, C. Fabre, J. M. Janot, E. J. Land, S. Leach, V. Leboulaire, A. Rassat, S. Roux and P. Seta, *Chem.–Eur. J.*, 1998, **4**, 270–278.
67 J. N. Demas and G. A. Crosby, *J. Phys. Chem.*, 1971, **75**, 991.
68 R. F. Kubin and A. N. Fletcher, *Chem. Phys. Lett.*, 1983, **99**, 49.

69 S. J. K. Pond, M. Rumi, M. D. Levin, T. C. Parker, D. Beljonne, M. W. Day, J. L. Bredas, S. R. Marder and J. W. Perry, *J. Phys. Chem. A*, 2002, **106**, 11470–11480.
70 M. Rumi, J. E. Ehrlich, A. A. Heikal, J. W. Perry, S. Barlow, Z. Y. Hu, D. McCord-Maughon, T. C. Parker, H. Rockel, S. Thayumanavan, S. R. Marder, D. Beljonne and J. L. Bredas, *J. Am. Chem. Soc.*, 2000, **122**, 9500–9510.
71 C. Xu and W. W. Webb, *J. Opt. Soc. Am. B*, 1996, **13**, 481–491.
72 C. Xu, R. M. Williams, W. R. Zipfel and W. W. Webb, *Bioimaging*, 1996, **4**, 198.
73 M. Albota, D. Beljonne, J. L. Bredas, J. E. Ehrlich, J. Y. Fu, A. A. Heikal, S. E. Hess, T. Kogej, M. D. Levin, S. R. Marder, D. McCord-Maughon, J. W. Perry, H. Rockel, M. Rumi, C. Subramaniam, W. W. Webb, X. L. Wu and C. Xu, *Science*, 1998, **281**, 1653–1656.
74 P. A. Padmawar, J. E. Rogers, G. S. He, L. Y. Chiang, L. S. Tan, T. Canteenwala, Q. D. Zheng, J. E. Slagle, D. G. McLean, P. A. Fleitz and P. N. Prasad, *Chem. Mater.*, 2006, **18**, 4065–4074.
75 Y. M. Zhao, Y. Shirai, A. D. Slepkov, L. Cheng, L. B. Alemany, T. Sasaki, F. A. Hegmann and J. M. Tour, *Chem.–Eur. J.*, 2005, **11**, 3643–3658.
76 G. P. Zhang, X. Sun and T. F. George, *J. Phys. Chem. A*, 2009, **113**, 1175–1188.
77 J. L. Li, S. F. Wang, H. Yang, Q. H. Gong, X. An, H. Y. Chen and D. Qiang, *Chem. Phys. Lett.*, 1998, **288**, 175–178.
78 K. I. Salokhiddinov, I. M. Byteva and G. P. Gurinovich, *J. Appl. Spec.*, 1981, **34**.
79 R. Schmidt and H.-D. Brauer, *J. Am. Chem. Soc.*, 1987, **109**.
80 P. Bilski, B. Z. Zhao and C. F. Chignell, *Chem. Phys. Lett.*, 2008, **458**, 157–160.
81 F. Prat, R. Stackow, R. Bernstein, W. Y. Qian, Y. Rubin and C. S. Foote, *J. Phys. Chem. A*, 1999, **103**, 7230–7235.
82 D. I. Schuster, S. MacMahon, D. A. Guldi, L. Echegoyen and S. E. Braslavsky, *Tetrahedron*, 2006, **62**, 1928–1936.
83 Y. Rio, G. Accorsi, H. Nierengarten, C. Bourgogne, J. M. Strub, A. Van Dorsselaer, N. Armaroli and J. F. Nierengarten, *Tetrahedron*, 2003, **59**, 3833–3844.
84 J. Issberner, F. Vogtle, L. DeCola and V. Balzani, *Chem.–Eur. J.*, 1997, **3**, 706–712.
85 J. W. Arbogast, A. P. Darmanyan, C. S. Foote, Y. Rubin, F. N. Diederich, M. M. Alvarez, S. J. Anz and R. L. Whetten, *J. Phys. Chem.*, 1991, **95**, 11–12.
86 R. V. Bensasson, E. Bienvenue, M. Dellinger, S. Leach and P. Seta, *J. Phys. Chem.*, 1994, **98**, 3492–3500.
87 T. Galili, A. Regev, H. Levanon, D. I. Schuster and D. A. Guldi, *J. Phys. Chem. A*, 2004, **108**, 10632–10639.